Accepted Manuscript

Re(I) tricarbonyl complex of 1,10-phenanthroline-5,6-dione: DNA binding, cytotoxicity, anti-inflammatory and anti-coagulant effects towards Platelet Activating Factor

Michael Kaplanis, George Stamatakis, Vasiliki D. Papakonstantinou, Maria Paravatou-Petsotas, Constantinos A. Demopoulos, Christiana A. Mitsopoulou

Please cite this article as: Michael Kaplanis, George Stamatakis, Vasiliki D. Papakonstantinou, Maria Paravatou-Petsotas, Constantinos A. Demopoulos, Christiana A. Mitsopoulou, 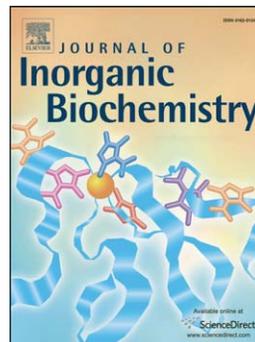Re(I) tricarbonyl complex of 1,10-phenanthroline-5,6-dione: DNA binding, cytotoxicity, anti-inflammatory and anti-coagulant effects towards Platelet Activating Factor, *Journal of Inorganic Biochemistry* (2014), doi: 10.1016/j.jinorgbio.2014.02.003

Re(I) tricarbonyl complex of 1,10-phenanthroline-5,6-dione: DNA binding, cytotoxicity, anti-inflammatory and anti-coagulant effects towards Platelet Activating Factor.

Michael Kaplanis [a], George Stamatakis [b], Vasiliki D Papakonstantinou [b], Maria Paravatou-Petsotas [c], Constantinos A. Demopoulos [b], Christiana A. Mitsopoulou [a], *

[a]. Laboratory of Inorganic Chemistry, Faculty of Chemistry, National and Kapodistrian University of Athens, Panepistimiopolis Zografou, 157 71 Athens, Greece

[b]. Laboratory of Biochemistry, Faculty of Chemistry, National and Kapodistrian University of Athens, Athens 15771, Greece

[c]. Institute of Nuclear and Radiological Sciences and Technology, Energy and Safety, National Centre for Scientific Research ''Demokritos'', 15310 Athens, Greece

Abstract

The complex *fac*-[Re(CO)$_3$(phendione)Cl] (**1**) (where phendione=1,10-phenanthroline-5,6-dione) has been synthesized and fully characterized by UV-visible, FTIR, and NMR techniques. The DNA binding properties of **1** are investigated by UV-spectrophotometric (melting curves), covalent binding assay, CV (cyclic voltammetry), circular dichroism (CD) and viscosity measurements. Experimental data indicate that **1** fits into the major groove without disrupting the helical structure of the B-DNA in contrast to the free phendione which intercalates within the base pairs of DNA. Upon irradiation, complex **1** promotes the cleavage of plasmid pBR322 DNA from supercoiled form I to nicked form II via a proton coupled electron transfer mechanism. This comes as a result of experimental data in anaerobic /aerobic conditions and in the presence of DMSO. The biological activities of **1** and its precursors [Re(CO)$_5$Cl] and phendione are tested towards a series of cancerous cell lines as glioblastoma (T98G), prostate cancer (PC3) and breast cancer (MCF-7) as well as platelet activating factor (PAF)-aggregation. Moreover, all the aforementioned compounds are tested for their ability to modulate PAF-basic metabolic enzymes activities in preparations of rabbit leukolytes. The *in vitro* experiments indicate that phendione has a better antitumor effect than cisplatin whereas [Re(CO)$_5$Cl] is a better PAF inhibitor than both the phendione ligand and **1**. Moreover, for the first time it is indicated that [Re(CO)$_5$Cl], with a IC$_{50}$ of 17 nM is comparable to the widely used PAF receptor antagonists, BN52021 and WEB2170 with IC$_{50}$ of 30 and 20 nM, respectively, whereas **1** affects PAF-catabolism.

*Corresponding author: Email: cmitsop@chem.uoa.gr; Fax: +30210 7274435

1. Introduction

The antitumor activity of cisplatin and its associated side effects and resistance continue to fuel research in organometallic complexes in an effort to formulate new, specific metallodrugs with fewer or no side effects [1]. In this context, transition metal complexes are studied for their efficient DNA binding ability [2-6] and it is well documented that they can be used as probes capable to utilize nucleic acid structures [2-6], DNA-molecular light switches [7,8], oxidative cleaving agents for DNA [4-6,8], and potential anti-cancer drugs [9-11]. Rhenium belonging in the same period as platinum have attracted researchers attention not only due to the 188-Re beneficial radiopharmaceutical activities but also because several Re(I) complexes were found to be very active against suspended cancer cell lines (as MOLT-4 and HL-60) and solid tumors like MCF-7 and SK2 [12]. Moreover, significant cancer cell cytotoxicity has been reported for rhenium (I) tricarbonyl complexes [13,14] whereas a plenty of Re(I) polypyridine complexes have been designed not only for targeting biomolecules, such as DNA [8,15-20] and protein [9,21,22] but also as cellular probes with cellular uptake like cytotoxicity and bioimaging application [9,22].

On the other hand, the coordinated ligand of a complex plays an important role since it controls the way the complex interacts to DNA; this can occur by intercalation, groove binding or external electrostatic binding [2-4]. An interesting class of ligands is phenanthrolines and substituted derivatives which interact with DNA by aromatic π stacking between the base pairs, both when they are free or coordinated to a metal centre. Among the phenanthroline derivatives, 1,10-phenanthroline-5,6-dione (phendione), displays significant anticancer role with and without a coordinated metal [23,24], whereas it also displays antibacterial and antifungal activity [23-27]. Actually, its biological activity is enhanced or reduced when it is coordinated to different metal centers [27, 28] even if it keeps its planar geometry, indicating that the role of the metal moiety is crucial for the electronic properties both of the metal center and the phendione resulting in significant differences in biological activity. Recently, the anticancer activity of phendione and its Cu^{2+} and Ag^+ complexes has been studied in a wide spectrum of cell lines, containing not only mouse's and monkeys' cells, but also human-derived cancer cell lines [23,24,26]. In the majority of cases, these complexes exhibit excellent biological activity and represent a class of DNA-targeting compounds capable of inhibiting nucleotide synthesis. In order to ascertain the likely cyto-selective nature of these agents, C. Deegan et al. [23] included two cell lines, both derived from normal human cells. The results suggest that these compounds are incapable of selectively killing cancer cells. Additionally, the metal complexes are more cytotoxic against all tested cell lines. Lately, it has been proved that the complex Pt(phendione)Cl$_2$ is as active as cisplatin against a variety of human cancer [27].

Little is known about the anti-inflammatory and anti-coagulant effects of Re(I) tricarbonyl complexes. Actually, in cancer, malignant situations such as angiogenesis and metastatic

progression are strongly promoted by the inflammatory tumor microenvironment due to the high levels of cytokine and chemokine secretion by the recruited inflammatory and stromal cells while coagulation of blood, inflammatory activation of platelets, endothelial cells and monocytes are typical steps in such cases. These occur as a common mechanistic effect of an inflammatory network of mediators like thrombin, platelet-activating factor etc [29,30].

Platelet activating factor (PAF), characterized mainly as 1-O-alkyl-2-acetyl-sn-glycero-3-phosphochloline, is an ether phospholipid mediator, synthesised and released by different types of cells, such as mast cells, neutrophils, monocytes, eosinophils, macrophages, platelets and endothelial cells. Its biological activity is exhibited through specific membrane PAF-receptors, coupled with G-proteins. The biosynthetic enzymes of PAF are PAF-cholinephosphotransferase (PAF-CPT, EC 2.7.8.16) and lyso PAF-acetyletransferase (lyso PAF-AT, EC 2.3.1.67), regulating PAF production in blood and cells. Concerning PAF catabolism, the basic enzyme of PAF degradation is PAF-acetylhydrolase (PAF-AH, EC 3.1.1.47), with its isoform in plasma also known as Lp-PLA$_2$ [31,32].

Studies have shown that transformed cancer cell lines able to express PAF-AH directly in the tumor microenvironment, reduced in growth and other malignant activities such as proliferation, motility and metastatic angiogenesis. This reduction was attributed to the blockage of PAF-induced signaling pathways. In addition, in patients with renal cell carcinoma treated with INF-a, a cytokine with anti-cancer activities, PAF-CPT activity was significantly reduced in comparison to those untreated [29].

Up to now, only organic compounds are used as PAF antagonists such as ginkolide BN 52012 and hetrazepines WEB 2170 whereas only recently the use of metal complexes has been referred as potential pharmaceutics against RAF activities [29].

In this study taking into consideration all the above, we examined for the first time the *in vitro* effects of phendione and its corresponding Re(I) complex against antitumor and PAF-induced biological activities. For this purpose, the antitumor activities of the aforementioned compounds were tested on three cell lines, namely human breast cancer MCF-7, human prostate cancer PC3 and human glioblastoma T98G and compared to cisplatin complex. The potent inhibitory effect of these compounds was studied on PAF-induced platelet aggregation towards washed rabbit platelets (WRPs). In addition, they were tested for their ability to modulate PAF-basic metabolic enzymes activities in preparations of rabbit leukolytes. Moreover, in an attempt to investigate the role of the metal centre on DNA binding mode of phendione, the interaction of the synthesized [Re(CO)$_3$(phendione)Cl] complex with calf thymus DNA was studied with a range of techniques whereas its photocleavage reaction on DNA was monitored by agarose gel electrophoresis.

2. Experimental

2.1. Materials and Methods

The chemicals and the solvents were purchased by Sigma Aldrich and used as received. Calf thymus DNA (CT-DNA) was purchased from Sigma. All the experiments involving interaction of the complexes with DNA were conducted in phosphate buffer (5 mM), pH = 7.00 and NaCl (4 mM). ^{1}H NMR spectra were recorded on a Varian Unity Plus 300 MHz spectrometer. Samples were run in a 5 mm probe with deuterated solvents as internal lock and reference. The assignment of the ^{1}H NMR spectra of the free ligand and complex is based on 2D NMR experiments (^{1}H–^{1}H COSY). Electronic absorption spectra were recorded on a Varian Cary 300E spectrometer at 25.0 ± 0.2 ^{o}C.

2.2. Synthesis

The ligand phendione was synthesized according to literature procedure [33] and was purified by crystallization from ethanol [34].

Synthesis of fac-[Re(CO)3(phendione)Cl] (*1*)

The complex **1** was synthesized based on the following report by Stoeffler [8] with some modifications [18]. A mixture of Re(CO)$_5$Cl (0.1211 g, 0.33 mmol) and phendione (0.1040 g, 0.50 mmol) were suspended in 5 mL toluene and refluxed under N$_2$ atmosphere for 4 h. Then, the mixture was allowed to cool to room temperature and the solid was collected by filtration under vacuum. The crude product was purified by column chromatography on silica gel using THF (tetrahydrofuran) as an eluent. THF evaporated under reduced pressure and the brown solid recrystallized from CH$_2$Cl$_2$ by the addition of diethyl ether. The NMR spectrum agrees well with the literature spectra. Yield: 74%. ^{1}H NMR (300 mHz, DMSO-d_6, δ ppm) 9.23 (d, 2H), 8.74 (d, 2H), 7.95 (t, 2H). FT-IR (cm^{-1}, KBr disc): 2033, 1910, 1891 ($\nu C \equiv O$), 1704 (νC=O). Anal. Calc. for C$_{15}$H$_6$N$_2$O$_5$ClRe: C, 34.72; H, 1.75; N, 5.40; found: 34.80; H, 1.72; N, 5.33

2.3. DNA binding studies

All experiments involving DNA interactions with complex **1** and its components were carried out in phosphate buffer pH=7.0 (the buffer was prepared by diluting 0.449g (3,3 mmol) of KH$_2$PO$_4$ and 0.296g (1.7 mmol) of K$_2$HPO$_4$ in 1 L of double distilled water containing NaCl 4mM). The ionic strength was 4 mM ensuring that the concentration of NaCl was at least 100-fold more than that of DNA. A solution of calf thymus DNA (CT-DNA) in buffer gave a ratio of UV absorbance at 260 and 280 nm of ca. 1.9:1, indicating that the DNA was sufficiently free of protein [35]. The DNA concentration per nucleotide was determined by UV absorption spectroscopy using the molar absorption coefficient (ε_{260} = 6600 M^{-1}cm^{-1}) at 260 nm [35]. Stock solution was stored at 4 ^{o}C and used within 4 days since at low concentrations DNA tends to absorb onto the surfaces of plastic tubes (from www.sigmaaldich.com). In all of our

5

experiments, the compounds and DNA are incubated for 24h at 25 °C since the equilibrium is very slow as it was found by UV-visible (UV-Vis) spectroscopy.

2.3.1. Thermal denaturation studies (T_m measurements)

Samples for thermal denaturation experiments were obtained by adding a freshly prepared solution of rhenium compound, dissolved in methanol, to a constant DNA concentration (15 μM) in phosphate buffer. The resulting solutions, (with ratios r= [complex]/ [DNA] = 0, 0.05 0.1, 0.2 and 0.5) were incubated for 24h at 25 °C, before measurements were recorded. DNA melting experiments were carried out by monitoring the absorbance of CT-DNA at 260 nm in the temperature range from 25.0 °C to 95.0 °C, on increasing temperature in 0.5 °C , with a Varian Cary 300 spectrophotometer. Samples were allowed to equilibrate for 1 min at each temperature. The melting temperature (T_m) of DNA was determined as the mid point of the optically detected transition.

2.3.2. Circular Dichroism (CD) measurements

CD measurements were carried out on a Jasco J700 spectropolarimeter interfaced with a PC. Data were analyzed through the standard Jasco software package. Each sample, which prepared similarity to T_m experiment ([DNA]=20 μM), was scanned in triplicate in a range of wavelengths between 200 nm to 400 nm. The drawn spectra are the means of three independent scans.

2.3.3. Cyclic Voltammetry (CV) experiment

CV measurements were carried out using a Pine AFCBP1 (pine Instrument Company, Groove City, PA, USA). The CV experiments were performed in a one compartment cell equipped with platinum working electrode, platinum wire as the auxiliary electrode and Ag/AgCl as reference electrode and the scan rate was 100 mV·s^{-1}. The potential was expressed as V *vs.* ferrocenium–ferrocene, and NaCl (10 mM) of the buffer was the supporting electrolyte.

2.3.4. Absorption titration

Absorption titration experiments were performed as follows: a constant metal complex concentration (20 μM) (dissolved in methanol) was incubated with varying nucleotide concentration (0-400 μM) in phosphate buffer solution (final percentage of MeOH = 5%). The data of the absorption titration experiments were fit in eq 1 to obtain intrinsic binding constant K_b,

$$[DNA]/(\varepsilon_a - \varepsilon_f) = [DNA]/(\varepsilon_b - \varepsilon_f) + 1/K_b(\varepsilon_b - \varepsilon_f) \tag{1}$$

where [DNA] is the concentration of DNA in base pairs, ε_a is the extinction coefficient of the observed absorption band at the given DNA concentration (correspond to A_{obs}/[complex]), ε_f is the extinction coefficient of the complex free in solution, and ε_b is the extinction coefficient of the

complex when fully bound to DNA. A plot of [DNA]/[ε_a - ε_f] versus [DNA] gave a slope 1/[ε_a - ε_f] and Y intercept equal to 1/K_b[ε_b - ε_f]. The intrinsic binding constant K_b is the ratio of the slope to the intercept. The linear least-squares analysis was done using Origin Lab 8.0.

2.3.5. Viscosity measurements

Viscometric experiments were performed using Schott Gerate AVS 310 Automated Viscometer, maintained at 25.0 ($\pm$0.1) ^{o}C in a thermostatic water bath. The concentration of DNA was 100 μM and that of metal complex was varied from 5 to 50 μM. Flow time of solutions in phosphate buffer (pH 7.0) was recorded in triplicate for each sample, and an average flow time was calculated. Data were presented as $(\eta/\eta_0)^{1/3}$ versus binding ratio r, where η is the viscosity of DNA in the presence of complex and η_0 is the viscosity of DNA alone. The relative viscosity of DNA in the presence and absence of the metal complex was calculated using the following expression: $\eta/\eta_0 = (t - t_0)/(t_{DNA} - t_0)$, where t_0 and t_{DNA} are the observed flow time of the buffer solution alone and DNA, respectively, while t the flow rate of the samples in the presence of the complex. The relationship between the relative solution viscosity (η/η_0) and contour length (L/L_0) is given by the equation $L/L_0 = (\eta/\eta_0)^{1/3}$, where L_0 denotes the apparent molecular length in the absence of the metal complex [36].

2.3.6. DNA electrophoresis

For the gel electrophoresis experiments, supercoiled pBR322 plasmid DNA (0.15 μg) was treated with different concentrations of complex **1** in 50 mM Tris·HCl and 18 mM NaCl buffer (pH= 7.2). The samples, which were incubated for 24 h in the dark at 25 ^{o}C, were irradiated for 2 h using 1000 W Xenon lamp (Oriel, mod 68820, Universal Arc. Lamp) and λ_{ir}> 335 nm. The samples were analyzed by electrophoresis for 1 h at 100 V on 1 % agarose gel in TBE (tris-borate-EDTA) buffer (89 mM Tris base, 89 mM boric acid, 2 mM EDTA, pH=8.0), followed by staining with ethidium bromide (0.5 μg/ mL final concentration). The gels were imaged with a BioSure UV-Transilluminator and photographed using a Picture Works, Photo Enhancer v3.2 digital camera.

2.4. In vitro cytotoxicity studies

2.4.1. Cell lines and culture conditions

Human cell lines of breast cancer (MCF-7), prostate cancer (PC3) and glioblastoma (T98G) were cultured in high glucose D-MEM medium with L-glutamine (Biochrom) supplemented with 10% foetal bovine serum (Biochrom) and penicillin/streptomycin (Biochrom) 10 U/mL / 10μg/mL. Cells were maintained at 37°C in a humidified 5% CO_2 incubator and were subcultured every 2-4 days.

2.4.2. Cytotoxicity of the ligand and the complexes (MTT assay)

7

In-vitro cytotoxicity studies were performed using the MTT (3-[4,5-dimethylthiazol-2-yl]-2,5 diphenyl tetrazolium bromide) colorimetric method, according to the literature [37,38]. Briefly, cells were seeded in 96-well flat-bottomed plates at a density of ~6000 cells per well and incubated for 24 h at 37 ^{o}C. The day after seeding, exponentially growing cells were incubated for 72 h with various concentrations of each compound. Cisplatin was added as positive control and wells with no metal compound as negative control. Tetraplicate wells were set up for each condition. After incubation the medium was removed and MTT solution (1 mg/mL in medium) was added for 4 hours. The resulting purple formazan crystals were dissolved by the addition of isopropanol (100 μL) and absorbance was measured for each well by a spectrophotometric [ELISA (enzyme- linked immunosorbent assay)] plate reader at 540 nm. Background absorption was measured at 620 nm and subtracted. The % cell viability was expressed as:

$$\% \text{ cell viability} = \frac{\text{mean OD of treated cells}}{\text{mean OD of untreaded cells (control)}} \times 100$$

The data were plotted against the corresponding compound concentration in a semi-log chart and the IC_{50} (the concentration causing 50% inhibition of cell proliferation) was determined from the dose–response curve, using GraphPad Prism 5.0. MTT assay was performed three independent times and in all experiments DMSO was lower than 1%.

2.5. PAF analysis

2.5.1 Materials and instruments

Centrifugations were performed on a Heraeus Labofuge 400R. Homogenizations were conducted in 30% of the power of a supersonic Bandelin Sonoplus HD 2070 sonicator (Heinrichstraze 3-4, D-12207 Berlin, Germany). The liquid scintillation counter used was a 1209 Rackbeta (Pharmacia, Wallac, Finland). Platelet aggregation studies were performed in a Chrono-Log model 400 VS aggregometer (Havertown, PA, USA) coupled to a Chrono-Log recorder at 37 °C with constant stirring at 1200 rpm.

BSA (bovine serum albumin), PAF (1-O-hexadecyl-2-acetyl-sn-glycero-3-phosphocholine), trichloroacetic acid (TCA), CDP-choline, lyso-PAF, acetyl-CoA, dithiothreitol (DTT), EDTA, MgCl₂, Tris HCl and analytical reagents were purchased from Sigma (St. Louis, MO, USA). 1-O-hexadecyl-2-[3H]acetyl-sn-glycerol-3-phosphocholine ([3H]-PAF) with a specific activity of 10 Ci/mmol was obtained from New England Nuclear (Dupont, Boston, MA, USA). 1-O-alkyl- 2-sn-acetyl-glycerol (AAG) was purchased from BIOMOL International LP (Palatine House, Matford Court, Exeter, UK). 2,5-Diphenyloxazole (PPO) and 1,4-bis(5-phenyl-2-oxazolyl) benzene (POPOP) were purchased from BDH Chemicals (Dorset, England). Scintillation liquid cocktail (dioxane base) was prepared by diluting 7 g PPO, 0.3 g POPOP and 100g Napthalene in 200 mL H₂O and then transferred to 1 L of dioxane. Liquid chromatography grade solvents and silica G for TLC were purchased from Merck KGaA (Darmstadt, Germany).

2.5.2 Isolation of plasma and leukocytes from blood samples

9 mL of blood were collected from the marginal ear vein of a white New Zealand rabbit in 1 mL of an anticoagulant solution of sodium citrate / citric acid. The sample was centrifuged at $630 \times g$ for 13 min at 25 ^{o}C. The supernatant of the centrifugation (plasma rich in platelets) was centrifuged at $1400 \times g$ for 20 min at 25 ^{o}C in order to obtain plasma. Saline was added in the pellet until the volume of 10 mL and mixed by inversion. The leukocytes were isolated after the sedimentation of the erythrocytes using 3.4 mL of dextran solution (3 % dextran in NaCl 0.15 M) for 1 h at room temperature. The leukocyte-rich supernatant was centrifuged at $500 \times g$ for 10 min at room temperature. The supernatant was removed and contaminating erythrocytes of the sediment pellet were lysed by the addition of 5 mL of a lysis solution consisted of 155 mM NH_4Cl, 10 mM $KHCO_3$, and 0.1 mM EDTA and then removed by centrifugation at $300 \times g$ for 10 min at room temperature. The isolated leukocytes were re-suspended in 1 mL of a buffer containing 50 mM Tris-HCl (pH 7.4), sonicated into ice (4 times of 15 s each) and centrifuged at $500 \times g$ for 10 min at 4 ^{o}C. Leukocytes homogenates after protein determination by Bradford method were aliquoted and stored at -80 ^{o}C.

2.5.3 Washed rabbit platelet aggregation assay

Biological assay on washed rabbit platelets was performed as previously described [31]. Briefly, PAF was dissolved in 12.5 mg of bovine serum albumin (BSA) per 1 mL of saline at a final concentration of 1.846 nM. The complexes and the ligand were tested in several concentrations, diluted when necessary in the BSA saline, for their ability to cause or inhibit platelet aggregation. After 1 minute of sample addition, stimulation with PAF (2.5×10^{-11} mol/L, final concentration in the cuvette) followed. The platelet aggregation induced by PAF was measured as PAF-induced aggregation, before (considered as 0% inhibition) and after the addition of various concentrations of the examined sample, creating a linear curve of percentage inhibition (ranging from 0 to 100%) versus different concentrations of the sample. From this curve, the concentration of the sample that inhibited 50% PAF induced aggregation was calculated, and this value was defined as IC_{50}.

2.5.4. PAF-CPT activity assay

The assay was performed on the homogenate of leukocytes isolated as previously described [39]. Briefly, the reaction was carried out at 37 ^{o}C for 20 min in a final volume of 200 μL containing 100 mM Tris-HCl (pH 8.0), 15 mM dithiothreitol (DTT), 0.5 mM EDTA, 20 mM $MgCl_2$, 1mg/ mL BSA, 100 μM CDP-Choline, 100 μM 1-O-alkyl-2-sn-acetyl-glycerol (AAG, added in the assay mixture in ethanol), and the sample (0.05 mg/ mL final concentration of protein). The mixture of Tris, DTT, EDTA, $MgCl_2$ and BSA was incubated in 37 ^{o}C for 5 min. Initially, the homogenate was added in the mixture. After 30 s, AAG was added and 30 s later the reaction was

started by addition of CDP-Choline. The reaction was stopped by adding 0.5 mL of cold methanol after 20 min.

2.5.5. Lyso-PAF-AT activity assay

The assay was performed on the homogenate of leukocytes isolated from New Zealand White rabbits as previously described. Briefly, the reaction was carried out at 37 $^{\circ}$C for 30 min in a final volume of 200 μL containing 50 mM Tris-HCl (pH 7.4), 0.25 mg/ mL BSA, 20 μMM lyso-PAF and 200 μM acetyl-CoA and the sample (0.125 mg/ mL final concentration of protein). The reaction started by the addition of the homogenated sample and was stopped after 30 min by adding 0.5 mL of cold methanol.

2.5.6. Determination of produced PAF and biosynthetic enzymes (PAF-CPT and lyso-PAF-AT) activities

The extraction, purification and determination of the produced in each assay PAF was carried out as previously described [39]. Briefly, PAF was extracted according to the Bligh–Dyer method and was separated by thin-layer chromatography (TLC) on Silica Gel G coated plates with a development system consisting of chloroform:methanol:acetic:acid:water (100:57:16:8, v/v/v/v). PAF bands were scrapped off, extracted and the amount of PAF was determined by the washed rabbit platelet aggregation assay. All assays were performed in triplicate and specific activities of PAF-CPT and lyso-PAF-AT were expressed as pmol of produced PAF/min/mg of sample protein present in each assay.

2.5.7. Plasma PAF-AH (LpPLA2) activity assay

Plasma PAF-AH was determined in rabbit plasma by the trichloroacetic acid precipitation method using [3H] PAF as a substrate, as previously described [39]. Briefly, 2 μL of plasma were incubated with 4 nmol of [3H]-PAF (20 Bq per nmol) for 30 min at 37 $^{\circ}$C in a final volume of 200 μL of 50 mM Tris/HCl buffer (pH 7.4). The reaction was terminated by the addition of BSA solution (final concentration 0.75 mg/mL) and followed by precipitation with trichloroacetic acid (TCA final concentration 9.6% v/v). The samples were placed in an ice bath for 30 min and subsequently centrifuged at 16000×g for 5 min at 4 $^{\circ}$C. The [3H]-acetate released into the aqueous phase was measured on a liquid scintillation counter. All assays were performed in triplicate and the enzyme specific activity was expressed as pmol of degraded PAF/min/μL of plasma.

3. Results and discussion

3.1. Synthesis and characterization

The Re(I) complex was synthesized according to the general method reported by Ruiz et al [18] with some modifications. The preparation included the reaction of the precursor [Re(CO)$_5$Cl] with slight excess of the ligand phendione (1:1.2) under reflux in toluene for 4 h. The crude product was purified using column chromatography on silica gel and the red band recrystallized from CH$_2$Cl$_2$ by the addition of ether. In Table S1 (supporting material) are reported the proton chemical shifts of phendione and the corresponding Re(I) complex, and are compatible with those of the literature [8,18,33,34]. The deshielding of the diimine protons can attributed to the electron density's removal from phendione towards [Re(CO)$_3$Cl] core after complexation [40].

Please insert here Fig 1.

The IR spectra, recorded in KBr pellets, are rather complicated but despite this, there are some features quite common to aromatic rings corresponded to the stretches of C–H and C–C and the out of plane bending of C–H. The most characteristic band of the phendione appears at 1687 cm^{-1} and assigned as v(C=O). The corresponding band for complex **1** appears at 1704 cm^{-1}. The characteristic peaks of complexes of the type *fac*-[Re(α-diimine)(CO)$_3$Cl] observed in the region 1890 – 2040 cm^{-1}, due to the $C \equiv O$ stretching vibrations. For **1**, the highest band appears at 2033 cm^{-1} and corresponds to a totally symmetric in-phase v(CO) vibration. The two lower bands belong to the out of-phase totally symmetric vibration and the asymmetric vibration of the equatorial CO ligands, and for **1** appear at 1891 and 1910 cm^{-1}, respectively [41].

Electronic absorption spectra of complex **1** in various solvents with different polarity are indicated in Fig. 2. The spectrum consists of two main bands; a broad low-energy band and a narrower, more intense, high-energy band at the UV region. The UV bands resemble in shape and position the lowest-energy ones in the corresponding spectrum of the free diimine ligand, despite they are found at higher wavelengths and are more structured. The shape along with the position and the solvent dependence of the low-energy band denote its (Re)d$\pi \rightarrow \pi$*(phendione) charge-transfer (MLCT) character, which agrees with previous interpretations of many mononuclear tricarbonyl Re complexes [41,42]. From Fig. 2 it is obvious that the polarity of the solvent affects the shape and the place of the bands not only because of the solvatochromic effect but also due to the hydrogen bonds that the oxygen atoms of the phendione can form. To the existence of these bonds can be attributed the observed changes over time to the UV-Vis of complex **1** in methanolic buffer solution. (Fig. S1). This is further supported by the ^{1}H-NMR experiments in a mixture of 10% CD$_3$OD and 90% D$_2$O that shows substantial line broadening. This behaviour also suggests that complex **1** is in equilibrium with a hydrated species. The hydration reaction occurs in carbonyl groups, when the ligand coordinate to a metal centre or a proton ion binds to the nitrogen atoms of the phendione [43]. Indeed, this hydration observed for complexes [Os(bpy)$_2$(phendione)]$^{2+}$ [43]

and for $[Ru(phen)_2(phendione)]^{2+}$ [44], with the latter to be responsible for the photocleavage of supercoiled pUC18 plasmid DNA [44].

Please insert here Fig 2.

3.2. DNA binding studies

3.2.1 T_m measurements

DNA thermal denaturation experiments show only a minor shift in the DNA melting temperature (T_m), giving ΔT_m values of 1-3 ^{o}C upon addition of the complex **1** to CT- DNA (Table 1). Particularly, a relative low destabilization of the double helix is observed at the ratio 0.5 (r = [complex]/ [DNA]) with ΔT_m= 2.9 ^{o}C. The data suggest a primarily external or groove binding nature of the complex. Non classical intercalating complexes show similar behaviour [45-47], while intercalating ligands like ethidium bromide show significantly high ΔT_m values [48].

Please insert here Table 1.

3.2.2. Circular dichroism experiments

The CD spectral technique is useful in monitoring the conformational variations of DNA in solution. CD of native CT-DNA is conservative, giving a negative band at ~246 nm, arising due to the B-form right handed helicity, and a positive band at ~278 nm originating from uniform nucleobase stacking in the B-form conformation [49]. Both intensities and wavelengths are quite sensitive to the mode of the interaction with small molecules. It is generally accepted that the groove binding or electrostatic interaction does not change significantly the intensities of both the bands, while the classical intercalation enhances the intensities due to the strengthening of the base-stacking and stabilization of the right-handed B conformation.

Upon addition of the rhenium(I) complex no significant modification is observed either to the ellipticity of the bands or to their position (Fig. S2). Particularly, only a little change in ellipticity at 278 nm ($\Delta\varepsilon$ decrease from 1.82 to 1.55 $M^{-1}cm^{-1}$) and at 248 nm is observed, for the ratio r = 0.2, as shown in Table 1, whereas there is no observable change at the wavelength of the two bands.

The results suggest that the complex cannot change the conformation of the B-form of DNA, and this is a first clue, that its mode of binding to DNA is not intercalative in nature, in accordance with the T_m measurements. Recently, molecular modelling studies of $[Co(phendione)_2Cl_2]^+$, shows that although it covalently binds to N7 of guanine, the ligand fits into the major groove without disrupting the helical structure of the B-DNA [50].

12

3.2.3. CV studies

Electrochemical investigation of complex-DNA interactions can provide a useful complement to other methods and yield information about the mechanism of the interaction [51,52]. Thus, Fig. 3 shows the cyclic voltammograms of the complex **1** (100 μM) at the absence and presence of CT-DNA (200 μM). After addition of DNA to the complex no new redox peaks appeared, but the current intensity of all the peaks decreased, suggesting the existence of an interaction between **1** and CT-DNA, and can be explained in terms of an equilibrium mixture of free and DNA-bound complex to the electrode surface [52]. From Fig. 3, is observed that in the presence of DNA, the cathodic potential E_{pc} shows a negative shift up to -313 mV (ΔE_{pc}= -44 mV), while the anodic peak E_{pa} presents a decrease of the current intensity with no shift to its potential. The negative shift of the cathodic potential may suggest the external binding of the complex to DNA.

Please insert here Fig 3

3.2.4. Absorption titration

The interaction of small molecules with DNA can be investigated by absorption titration. Complexes that bound to DNA by intercalation usually cause a decrease in absorbance (hypochromism) and a red shift (bathochromism) to the wavelength at 310nm involving a strong π-π^* stacking interaction between aromatic chromophore and the base pairs of DNA. The extent of hypochromism and bathochromism depends on intercalative binding strength [53,54]

Electronic absorption spectra of the complex **1** (constant concentration at 20 μM) in phosphate buffer pH=7 is indicated in Fig. 4. Upon addition of DNA, complex exhibits decrease in absorption at 310 nm (hypochromism) around to 30%. Despite the observable hypochromism, the interaction is not intercalative in nature, as suggest the negligible shift in the absorption maximum wavelength. This behaviour agrees with a groove binding mode.

To analyze quantitatively the binding strength of complex **1**, the intrinsic binding constant K_b of **1** with DNA was obtained by monitoring the intense of the absorbance at 310 nm of **1** with increasing concentration of DNA and by using eq 1. The value of the K_b, which is given as a ratio of slope to y intercept obtained from the plot of [DNA]/(ε_a-ε_f) *vs.* [DNA] (inset Fig. 4), was determined as $7.95(\pm1.89)\times10^4$ M^{-1}. As was expected, the binding affinity with DNA is smaller than classic intercalating complexes with dppz ligand, such as [Ru(bpy)$_2$dppz]$^{2+}$ (5.0×10^6 M^{-1}), [Ru(phen)$_2$dppz]$^{2+}$ (5.1×10^6 M^{-1}) [54]. Complex **1** has a smaller K_b value than the related Re(I) complexes with an intercalative ligand (such as dppz) [8,16,20], due to the non-intercalative mode of the phendione ligand.

Complex **1** exhibits a weak luminescence in phosphate buffer. Binding of **1** to CT-DNA did not lead to any change in its emission intensities. Thus, emission spectroscopy could not be used to examine the binding properties of the complex.

13

Please insert here Fig 4

3.2.5. Viscosity measurements

Optical photophysical probe provides necessary but not sufficient clues to support binding modes, whereas hydrodynamic measurements that are sensitive to the length change are regarded as the most critical tests of a binding model in solution. For example, a classical intercalator, such as ethidium bromide, causes a significant increase in viscosity of a DNA solution because of the separation of the base pairs at the intercalation site, and hence, the expansion of the DNA molecular length. In contrast, a ligand that binds in the DNA grooves causes less-pronounced changes or no change in viscosity of a DNA solution [55,56]. Fig. 5 indicates the relative viscosity of DNA ([DNA]=100 μM) in the presence of varying amounts of complex **1.** The flow time of each sample was recorded in triplicate, and each value did not differ from each other more than 0.4 s. The observed decrease of the relative viscosity (up to 0.92) reveals that complex **1** interacts with groove or electrostatic binding mode, which can bent (or kink) the DNA helix reducing its effective length and concomitantly its viscosity. The Δ isomer of the groove binder $[Ru(phen)_3]^{2+}$ causes a similar decrease of the relative viscosity of DNA [55].

Please insert here Fig 5.

3.2.6. Gel Electrophoresis of Re(I) complex

The ability of complex **1** to cleave DNA upon irradiation was determined by agarose gel electrophoresis. Thus, supercoiled pBR322 DNA was incubated with different concentration of **1** (0-100 μM) and the samples was irradiated with $\lambda_{ir}> 335$ nm for 2 h under aerobic conditions. The results indicate (Fig. 6) that complex **1** promotes the single strand cleavage of the supercoiled (Form I) to nicked DNA (Form II). The untreated plasmid DNA (lane 1) does not show any cleavage upon irradiation. However, with increasing concentration of **1** (lanes 2-4) the amount of Form II increases gradually, whereas that of Form I diminishes. No DNA cleavage was observed upon incubation of DNA with **1** in the dark (lane 5).

The precursor mechanistic studies revealed that complex **1** can photocleave DNA under both aerobic (lane 2-4) and anaerobic conditions (lane 7), with somewhat less cleavage yields without O_2 and under argon atmosphere (lane 7). In the anaerobic experiment, the sample was subjected to three consecutive freeze-pump-thaw cycles, incubated for 24h under argon atmosphere and then irradiated. The data in lane 7 reveal that an oxygen independent pathway exists but the enhanced photocleavage activity of **1** in the presence of oxygen indicates that $[Re(CO)_3(phendione)Cl]$ can also induced DNA damage by the generation of ROS. Since DMSO is

known to quench hydroxyl radicals, experiments in the presence of it were performed (lane 6) indicating no attenuation of the photocleavage reaction. As a consequence and taking into consideration the anaerobic photoinduced cleavage of DNA a mechanism via a proton coupled electron transfer could be suggested, similar to the well documented mechanism of the cleavage of the complex $[Ru(phen)_2phendione]^{2+}$ [44].

Please insert here Fig 6.

3.3. Cytotoxicity studies

In an attempt to elucidate the role of the metal centre when coordinated with the ligand phendione, we determined the cytotoxicity properties of complex **1**, the precursor molecule $Re(CO)_5Cl$ and the phendione ligand, against three human cancer cell lines, glioblastoma (T98G), prostate cancer (PC3) and breast cancer (MCF-7) cells using the MTT assay. As a positive control was used cisplatin.

The IC_{50} values shown in Table 2, indicate that phendione is toxic against T98G (IC_{50}=4.91 μM), PC3 (IC_{50}=3.01 μM) and MCF-7 (IC_{50}=2.45 μM) cell lines even more than cisplatin and confirm previous published results referring the toxicity of phendione in various cell lines [23,26,27]. The limited solubility of the complex **1** in aqueous medium did not allow the evaluation of the IC_{50} values [57]. Complex **1** is not active in 10 μM (data not shown). However, in 50 μM concentration of **1** (Fig. 7) the cell viability decreases with respect to the control at least 45%, 40% and 27% for MCF-7, T98G and PC3 cells, respectively. It is worth noting that the starting material $Re(CO)_5Cl$ reduces the cell viability about 50% only at 200 μM (Fig. S4). The high cytotoxicity of phendione ligand is reduced when the ligand coordinates with Re(I) core for all cell lines tested.

Similar to our results, a significant decrease in cytotoxicity observed when phendione coordinate with platinum. Roy et al. [27] have proved that coordination of this ligand led to a decrease in cytotoxicity, reducing it from 1.4-fold against A2780R, to almost 7-fold against the lung cancer cell line (H226). Nevertheless, according to our results, the Re(I) centre seems to reduce the cytotoxic activity of the free ligand more than the Pt(II) centre, since $Pt(phendione)Cl_2$ has comparable IC_{50} values to cisplatin. Recently, it was referred that the Re(I) complex with appt (appt=2-amino-4-phenylamino-6-(2-pyridyl)-1,3,5-triazine]), which interacts to DNA with minor groove bindings, has moderate cytotoxicity against several cancer cells (IC_{50}= 50 μM against HeLa), while it is non toxic against noncancerous normal lung fibroblasts [58]. Taking into account all the above, we could conclude that the metal centre seems to play an important role and the rhenium(I) centre reduces the toxic effect, at least with that ligand.

Please insert here Table 2 and Fig. 7

3.4 PAF assays

3.4.1. Inhibitory effect of Re(I) metal complexes and phendione towards the PAF induced WRP's aggregation.

All compounds under investigation inhibited the PAF-induced aggregation of WRPs. This inhibitory effect is expressed by their IC_{50}, since a low IC_{50} value reveals stronger inhibition of the PAF-induced aggregation for a given compound concentration. The IC_{50} values of the samples tested against PAF induced platelet aggregation are presented in Table 2. The IC_{50} values are comparable to the ones achieved from the best specific PAF receptor inhibitors like BN 52021 [59]. The interesting observation from these data is that the initial complex [Re(CO)$_5$Cl] with an IC_{50} value of 170 ± 90 nM is better PAF inhibitor than both the phendione ligand and complex **1** with IC_{50} values of 925 ± 130 nM and 862 ± 150 nM, respectively. These observations indicate that coordination of phendione to metal core tricarbonyl-Re(I) enhances its inhibitory effect towards the PAF-induced rabbit PRP aggregation but at the same time the phendione-metal coordination reduces the inhibitory action of the [Re(CO)$_5$Cl] complex. The later is in contrast with previous data where coordination of a ligand to a metal ion enhances the inhibitory activity towards PAF-aggregation of both the initial starting compounds –ligand and metallic moiety-e.g when organometallic moieties of Re coordinates to tamoxifen [60].

Please insert here Fig. 7

3.4.2. Effect of Re(I) metal complexes towards the PAF-basic metabolic enzymes.

In order to determine the possible interactions between the two metal complexes under study and PAF metabolism, the in vitro effect of these compounds on the activities of PAF-basic metabolic enzymes lyso-PAF-AT and PAF-CPT was also studied (Fig. 8 and 9). The choice to study these effects on the PAF-main enzyme activities on rabbit leukocytes homogenates depends on a) the ease of these cells to be handled and separated b) the finding that they are the main contributors of PAF-synthesis in blood in comparison to platelets or red blood cells and c) their participation in inflammatory procedures and manifestations in different diseases, also through their ability to produce PAF. We have found that both the Re (I) complexes affect PAF biosynthesis (Fig. 8 and 9), namely PAF-CPT and lyso-PAF-AT, and also its main catabolic enzyme, Lp-PLA2, (Fig. 10). Interestingly, the effects of the two complexes differed between the two PAF biosynthetic enzymes. The [Re(CO)$_5$Cl] complex greatly inhibits PAF-CPT activity while it increases lyso-PAF AT activity as shown in Figure 8. Actually, it exhibits a very potent inhibitory effect towards PAF-CPT (Fig 8) achieved even from the lowest concentration tested and remained stable for the full

16

concentrations' range. Taking into account that this complex also exhibits one of the most potent anti-PAF effects in platelets, its additional inhibitory effect towards PAF-biosynthesis provide new anti-inflammatory potentials for this compound.

On the other hand, complex **1** exhibits a small inhibitory effect against lyso-PAF AT that remained stable for all the concentrations tested. This complex increases PAF-CPT activity at low concentrations, an effect that is reduced at the higher concentrations as shown in Figure 9.

Please insert here Fig. 8 and 9.

Both of the complexes increase Lp-PLA2 activity, with a more potent increment in the case of **1** which maintained a higher activity even in the higher concentration tested compared to [Re(CO)$_5$Cl]. The latter at a similar concentration returns to its basal level of activity (Figure 10).

Please insert here Fig. 10

4. Conclusions

In summary, from viscosity measurements, thermal denaturation and CV measurements it is observed that *fac*-[Re(CO)$_3$(phendione)Cl] binds with the grooves of the DNA double helix retaining its overall structure, whereas the un-coordinated ligand phendione interacts by intercalation to the DNA. The different way of the interaction of complex **1** and the corresponding ligand, namely phendione seems that reflects on their efficacy on various cancerous cell lines as glioblastoma (T98G), prostate cancer (PC3) and breast cancer (MCF-7). Actually, from the IC$_{50}$ values it is evident that phendione is extremely toxic against T98G (4.91 μM), PC3 (3.01 μM) and MCF-7 (2.45 μM) cell lines even more than cisplatin, whereas this cytotoxicity against all cell lines tested is almost completely lost when phendione ligand coordinates to Re(I). Complex **1** is active in 50 μM since in this concentration almost 45% human breast (MCF-7), 40% glioblastoma (T98G) and 27% prostate (PC3) cells are killed. It is worth noting that the starting material [Re(CO)$_5$Cl] is inactive at all tested cell lines even in very high concentrations (200 μM). On the other side, the coordination of phendione to the tricarbonyl Re(I) core has different results on the inhibitory effect towards PAF-induced aggregation of WRPs. Thus the initial complex [Re(CO)$_5$Cl] is better PAF inhibitor than both the phendione ligand and complex **1** indicating IC$_{50}$ values comparable to the ones achieved from the best specific PAF receptor inhibitors like BN 52021. Both these metal complexes exhibit also the ability to modulate in vitro the activities of PAF-basic biosynthetic enzymes, PAF-CPT and Lyso-PAF-AT, in the direction of down regulating PAF-levels, while only complex **1** seems to affect PAF-catabolism. Taking in consideration that PAF is key-mediator of the inflammatory malignant processes in different diseases the ability of the Re(I) complexes under

17

study to affect and directly interact with both the PAF/PAF-R and the key biosynthetic enzymes of PAF, provides a new perspective in the anti-malignant properties of these compounds. However, several *in vivo* studies must follow in order to confirm this *in vitro* interesting outcome. Moreover, complex **1** was found to promote the photocleavage of plasmid pBR322 DNA from supercoiled form I to nicked form II via a proton coupled electron transfer mechanism. This result according with its high affinity for DNA $[K=7.95(\pm1.89)*10^4 \text{ M}^{-1}]$ and its accessible photoexcited states in the visible region makes complex **1** a potential photodynamic therapy agent.

5. Abbreviations

AAG	1-O-alkyl- 2-sn-acetyl-glycerol
BN 5201	ginkolide
BSA	bovine serum albumin
appt	2-amino-4-phenylamino-6-(2-pyridyl)-1,3,5-triazine]
bpy	2,2'-bipyridine
CD	circular dichroism
CDP	cytidine diphosphate-choline
CV	cyclic voltammetry
CT-DNA	Calf Thymus DNA
dppz	dipyrido[2,3-a:2',3'-c]phenazine
DTT	dithiothreitol
ELISA	enzyme- linked immunosorbent assay
MCF-7	breast cancer
MTT	3-[4,5-dimethylthiazol-2-yl]-2,5 diphenyl tetrazolium bromidePAF
	Platelet activating factor
PAF-AH	PAF-acetylhydrolase
PAF-AT	PAF-acetyletransferase
PAF-CPT	PAF-cholinephosphotransferase
Lp-PLA$_2$	isoform of PAF-AH
PC3	prostate cancer
phen	1,10-phenanthroline
phendione	1,10-phenanthroline-5,6-dione
PRP	Rabbit platelet plasma
TBE	Tris-borate-EDTA
TCA	trichloroacetic acid

T98G	glioblastoma
THF	tetrahydrofuran
WEB 2170	hetrazepines
WRPs	Washed rabbit platelets

Acknowledgement

Appendix A: Supplementary data

UV-Vis of **1** in methanolic buffer solution (Figure S1), Circular dichroism measurements of the interaction of **1** with DNA (Figure S2), and % Cell Viability values of the precursor molecule [Re(CO)5Cl] (Figure S3).

19

References

[1] E. Wong, C.M. Giandomenico, Chem. Rev. 99 (1999) 2451-2466.

[2] K.E. Erkkila, D.T. Odem, J.K. Barton, Chem. Rev. 99 (1999) 2777-2796.

[3] C. Metcalfe, J.A. Thomas, Chem. Soc. Rev. 32 (2003) 215-224.

[4] J.A. Smith, M.W. George, J.M. Kelly, Coord. Chem. Rev. 255 (2011) 2666-5675.

[5] J.K. Barton, E.D. Olmon, P.A. Sontz, Coord. Chem. Rev. 255 (2011) 619-634.

[6] J.C. Genereux, J.K. Barton, Chem. Rev. 110 (2010) 1642-1662.

[7] A.E. Friedman, J.C. Chambron, J.P. Sauvage, N.J. Turro, J.K. Barton, J. Am. Chem. Soc. 112 (1990) 4960-4962.

[8] H.D. Stoeffler, N.B. Thornton, S.L. Temkin, K.S. Schanze, J. Am. Chem. Soc. 117 (1995) 7119-7128.

[9] K.K.W. Lo, K.Y. Zhang, S.P.Y. Li, Eur. J. Inorg. Chem. (2011) 3551-3568.

[10] K. Szacilowski, W. Macyk, A. Drzewiecka-Matuszek, M. Brindell, G. Stochel, Chem. Rev. 105 (2005) 2647-2694.

[11] L. Ronconi, P.J. Sadler, Coord. Chem. Rev. 251 (2007) 1633-1648.

[12] A. Quiroga, C. Ranninger, Coord. Chem. Rev. 248 (2004) 119-133.

[13] J. Zhang, J.J. Vittal, W. Henderson, J. Wheaton, I.H, Hall, Organomet. Chem. 650 (2002) 123-132.

[14] J. Ho, W.Y. Lee, K.J.T. Koh, P.P.F.Lee, Y.K.Yan, J. Inorg. Biochem. 119 (2013) 10-20.

[15] V.W.W. Yam, K.K.W. Lo, K.K. Cheung, R.Y.C. Kong, J. Chem. Soc., Chem. Commun. (1995) 1191-1193.

[16] V.W.W. Yam, K.K.W. Lo, K.K. Cheung, R.Y.C. Kong, J. Chem. Soc., Dalton Trans. (1997) 2067-2072.

[17] C. Metcalfe, M. Webb, J.A. Thomas, Chem. Commun. (2002) 2026-2027.

[18] G.T. Ruiz, M.P. Juliarena, R.O. Lezna, E. Wolcan, M.R. Feliz, G. Ferraudi, Dalton Trans. (2007) 2020-2029.

[19] E.D. Olmon, P.A. Sontz, A.M. Blanco-Rodríguez, M. Towrie, I.P. Clark, A. Vlček Jr, J.K. Barton., J. Am. Chem. Soc. 133 (2011) 13718-13730.

[20] F.L. Thorp-Greenwood, M.P. Coogan, L. Mishra, N. Kumari, G. Rai, S. Saripella, New J. Chem. 36 (2012) 64-72.

[21] K.K.W. Lo, K.H.K. Tsang, Organometallics 23 (2004) 3062-3070.

[22] K.K.W. Lo, M.W. Louie, K.Y. Zhang, Coord. Chem. Rev. 254 (2010) 2603-2622.

[23] C. Deegan, B. Coyle, M. McCann, M. Devereux, D. Egan, Chem. Biol. Interact. 164 (2006) 115-125.

[24] M. Devereux, D.O Shea, A. Kellett, M. McCann, M. Walsh , D. Egan, C. Deegan, K. Kedziora, G. Rosair, H. Muller-Bunz, J. Inorg. Biochem. 101 (2007) 881-892.

[25] B. Coyle, M. McCann, K. Kavanagh, M. Devereux, M. Geraghty, Biometals 16 (2003) 321-329.

[26] M. McCann, A.L.S. Santos, B.A. da Silva, M.T.V. Romanos, A.S. Pyrrho, M. Devereux, K. Kavanagh, I. Fichtner, A. Kellett, Toxicol. Res. 1 (2012) 47-54.

[27] S. Roy, K.D. Hagen, P.U. Maheswari, M. Lutz, A.L. Spek, J. Reedijk, G.P. van Wezel, ChemMedChem. 3 (2008) 1427-1434.

[28] S. Ghosh, A.C. Barve, A.A.Kumbhar, A.S. Kumbhar, V.G. Puranik, P.A. Datar, U. B. Sonawane, R. R. Joshi, J. Inorg. Biochem. 100 (2006) 331-343.

[29] A.B. Tsoupras, C. Iatrou, C. Frangia, C.A. Demopoulos, Infectious Disorders-Drug Targets 9 (2009) 390-399.

[30] V. Melnikova, M. Bar-Eli, Cancer Metastasis Rev. 26 (2007) 359-371.

[31] C.A. Demopoulos, R.N. Pinckard, D.J. Hanahan DJ., J. Biol. Chem. 254 (1979) 9355-9358.

[32] S. Antonopoulou, T. Nomikos, H.C. Karantonis, et al. PAF, a potent lipid mediator. In: Bioactive Phospholipids. Role in inflammation and Atherosclerosis. Tselepis AD (ed). Transworld Research Network, Kerala, India, 2008, p. 85-134

[33] M. Yamada, Y. Tanaka, Y. Yoshimoto, S. Kuroda, I. Shimao, Bull. Chem. Soc. Jpn. 65 (1992) 1006-1011.

[34] W. Paw, R. Eisenberg, Inorg. Chem. 36 (1997) 2287-2293.

[35] M.F. Reichmann, S.A. Rice, C.A. Thomas, P. Doty, J. Am. Chem. Soc. 76 (1954) 3047-3053.

[36] G. Cohen, H. Eisenberg, Biopolymers 8 (1969) 45-49.

[37] R. Supino, in: S.O'Hare, C.K. Atterwill (Eds.), Methods in Molecular Biology, vol. 43, Humana Press, Totowa, NJ, 1995, pp. 137-149.

[38] A. Bourkoula, M. Paravatou-Petsotas, A. Papadopoulos, I. Santos, H.J. Pietzsch, E. Livaniou, M. Pelecanou, M. Papadopoulos, I. Pirmettis, European J. Med. Chem. 44 (2009) 4021-4027.

[39] S. Antonopoulou, C.A.Demopoulos, C. Iatrou, G. Moustakas, P.Zirogiannis, Int. J. Biochem. 26 (1994) 1157-1162.

[40] I. Veroni, C.A. Mitsopoulou, F.J. Lahoz, J. Organomet. Chem. 693 (2008) 2451–2457.

[41] A. Vlcek Jr, Top Organomet. Chem. 29 (2010) 77-114.

[42] D.J. Stufkens, A. Vlcek Jr, Coord. Chem. Rev. 177 (1998) 127–179.

[43] Y. Lei, F.C. Anson, J. Am. Chem. Soc. 117 (1995) 9849−9854.

[44] S.A. Poteet, M.B. Majewski, Z.S. Breitbach, C.A. Griffith, S. Singh, D.W. Armstrong, M.O. Wolf, F.M. MacDonnell, J. Am. Chem. Soc. 135 (2013) 2419-2422.

[45] C.A. Mitsopoulou, C.E. Dagas, C. Makedonas, J. Inorg. Biochem. 102 (2008) 77-86.

[46] C.A. Mitsopoulou, C.E. Dagas, C. Makedonas, Inorg. Chim. Acta 361 (2008) 1973-1982.

[47] S. Saha, R. Majumdar, M. Roy, R.R. Dighe, A.R. Chakravarty, Inorg. Chem. 48 (2009) 2652-2663.

[48] A. Chouai, S.E. Wicke, C. Turro, J. Bacsa, K.R. Dunbar, D. Wang, R.P. Thummel, Inorg. Chem. 44 (2005) 5996-6003.

[49] V.I. Ivanov, L.E. Minchenk, A.K. Schyolki, A.I. Poletaye, Biopolymers 12 (1973) 89-110.

[50] S. Ghosh, A.C. Barve, A.A. Kumbhar, A.S. Kumbhar, V.G. Puranik, P.A. Datar, U.B. Sonawane, R.R. Joshi, J. Inorg. Biochem. 100 (2006) 331-343.

[51] C.A. Mitsopoulou, C. Dagas, Bioinorganic Chemistry and Applications Vol. 2010, Article ID 973742, 9 pages.

[52] G. Psomas, J. Inorg. Biochem. 102 (2008) 1798-1811.

[53] J.K. Barton, A.T. Danishshefsky, J.M. Goldberg, J. Am. Chem. Soc. 106 (1984) 2172-2176.

[54] A.E. Friedman, C.V. Kumar, N.J. Turro, J.K. Barton, Nucleic Acids Res. 19 (1991) 2595-2602.

[55] S. Satyanarayana, J.C. Dabrowiak, J.B. Chaires, Biochemistry 31 (1992) 9319-9324.

[56] S.S. Bhat, A.S. Kumbhar, P. Lonnecke, E. Hey-Hawkins, Inorg. Chem. 49 (2010) 4843-4853.

[57] S. Tzanopoulou, M. Sagnou, M. Paravatou-Petsotas, E. Gourni, G. Loudos, S. Xanthopoulos, D. Lafkas, H. Kiaris, A. Varvarigou, I.C. Pirmettis, M. Papadopoulos, M. Pelecanou, J. Med. Chem. 53 (2010) 4633-4641.

[58] D.L. Ma, C.M. Che, F.M. Siu, M. Yang, K.Y. Wong, Inorg. Chem. 46 (2007) 740-749.

[59] A.B. Tsoupros, A. Papakyriakou, C.A. Demopoulos, A.I. Philippopoulos, J. Inorg. Biochem. 120 (2013) 63-73.

[60] A. Vessiéres, S. Top, W. Beck, E. Hillard, G. Jaouen, Dalton Trans. 28 (2006) 529-541.

Table 1. Thermal Denaturation and circular dichroism measurements of DNA binding

studies of complex **1**.

	T_m measurements		Circular dichroism data	
	ΔT_m (^{o}C)	%hyp	λ (nm)	$\Delta\varepsilon$ (M^{-1}cm^{-1})
r=0	0	27.6	278	1.82
			246	-1.86
r=0.05	-1.62	27.8	278	1.82
			245	-1.97
r=0.1	-1.72	27.0	278	1.70
			247	-1.50
r=0.2	-0.76	19.0	279	1.55
			246	-1.97
r=0.5	-2.92	19.0	278	1.73
			245	1.93

24

Table 2. Cytotoxicity studies and inhibition of PAF induced platelet aggregation for cisplatin, phendione, complex (**1**) and the precursor molecule $Re(CO)_5Cl$. The IC_{50} values (μM) are represented as mean $\pm$ standard deviation.

Compound	Cytotoxicity studies			Inhibition of PAF
	T98G	PC3	MCF-7	
phendione	$4.91 \pm (2.06)$	$3.01 \pm (1.72)$	$2.45 \pm (0.71)$	$0.925 \pm (0.13)$
complex **1**	> 50	> 50	>50	$0.862 \pm (0.15)$
$Re(CO)_5Cl$	> 200	> 200	>200	$0.170 \pm (0.09)$
cisplatin	$6.45 \pm (1.64)$	$2.19 \pm (0.11)$	$11.06 \pm (2.49)$	$0.55 \pm (0.22)[a]$

a. from ref 59

Caption of Figures

Fig. 1. Structure of complex **1** and the corresponding phendione ligand.

Fig. 2. UV-Vis spectra of complex **1** in CH_2Cl_2, MeCN, MeOH

Fig. 3. Cyclic voltagramm of **1** (100 μM) in the absence (solid line) and in the presence of DNA (200 μM) (dashed line).

Fig. 4. Changes in the UV-Vis absorption spectra of complex **1** (20 μM) with increasing DNA concentrations. Arrow indicates the decreasing intensity of the 300nm band upon increasing [DNA]. The inset shows the plot of $-[DNA]/(\varepsilon_a-\varepsilon_f)x10^8$ *vs.* $[DNA]x10^5$ and the fit linear for the titration of DNA with **1**.

Fig. 5. Effect of increasing amounts of complex **1** (0–50 μM) on the relative viscosity of CT-DNA (100 μM).

Fig. 6. Agarose gel showing cleavage of pBR322 DNA (0.15 μg) incubated with different concentrations of complex **1** after irradiation at λ>335 nm. Lane 1: plasmid DNA only, Lane 2: DNA+10 μM of **1**, Lane 3: DNA+50 μM of **1**, Lane 4: DNA+100 μM of **1**, Lane 5: DNA+100 μM of **1** in the dark, Lane 6: DNA+100 μM of **1**+DMSO (0.9 M), Lane 7: DNA+100 μM of **1** deaerated.

Fig. 7. Effect of 50 μM of the tested compounds ($Re(CO)_5Cl$, complex **1**, ligand phendione, cisplatin) on % cell viability. Red, green and blue bars represent human glioblastoma, prostate and breast cancer cell lines respectively. The data are presented as mean (of three independent experiments) ± standard deviation. The errors of the compound $Re(CO)_5Cl$ and the complex 1 were about 3.5% and 5% at all tested cell lines, respectively. The error of the other compounds was lower than 1%.

Fig. 8. The effect of $Re(CO)_5Cl$ on specific activity of lyso PAF-AT (■) and specific activity of PAF-CPT (♦).

Fig. 9. The effect of complex **1** on specific activity of lyso PAF-AT (■) and specific activity of PAF-CPT (♦).

Fig. 10. The effect of $[Re(CO)_5Cl]$ (■) and complex **1** (♦) on the specific activity of Lp-PLA_2.
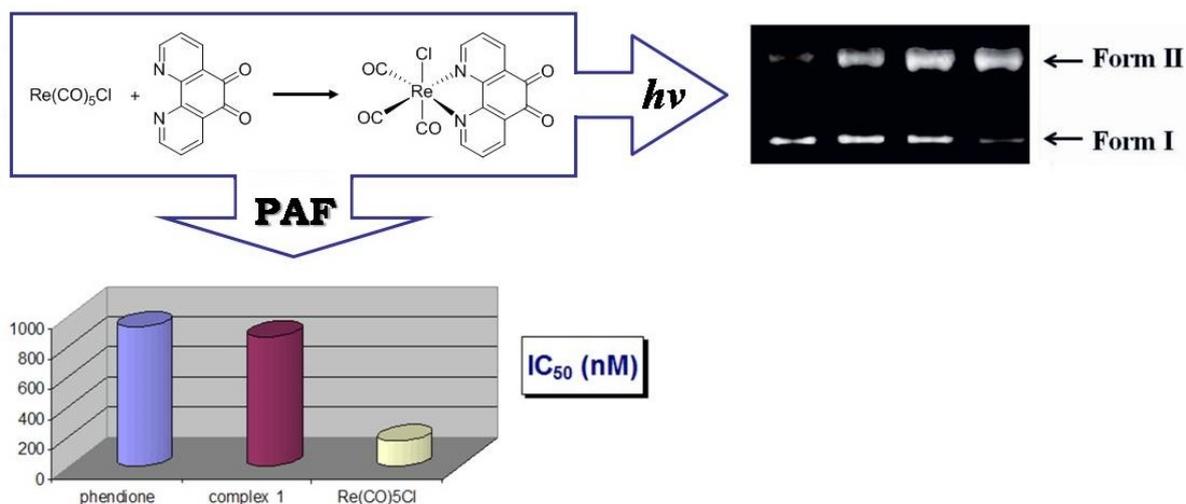
Graphical abstract (synopsis):

The affinity and mode of complex fac-[Re(CO)3(phendione)Cl] and its constituents [Re(CO)5Cl] and phendione binding to DNA, as well as their ability to cleave single-strand DNA were determined by physico-chemical techniques, whereas biological activities were derived from the cytotoxicity, platelet aggregation and enzyme inhibition assays.

f ac-Re(phendione)CO$_3$Cl (**1**)   phendione

Fig. 1

29
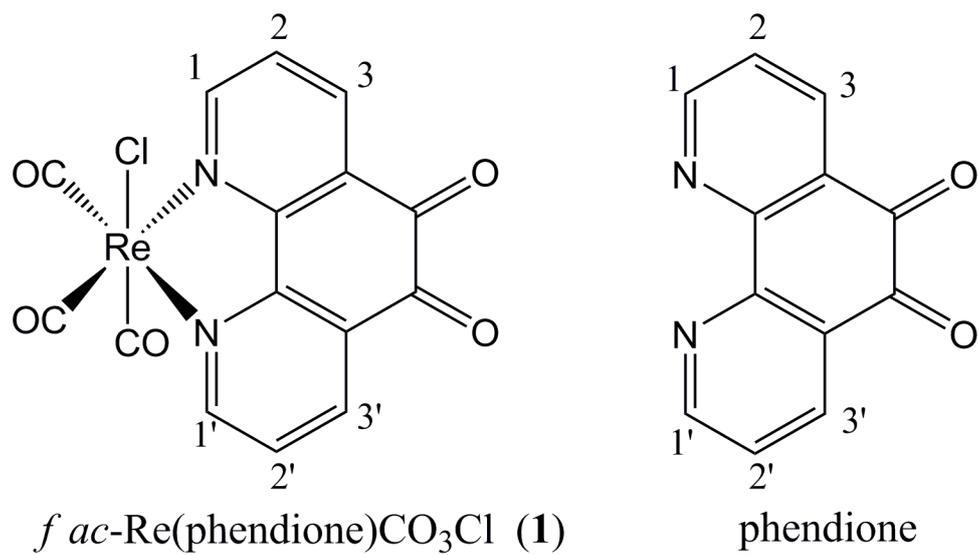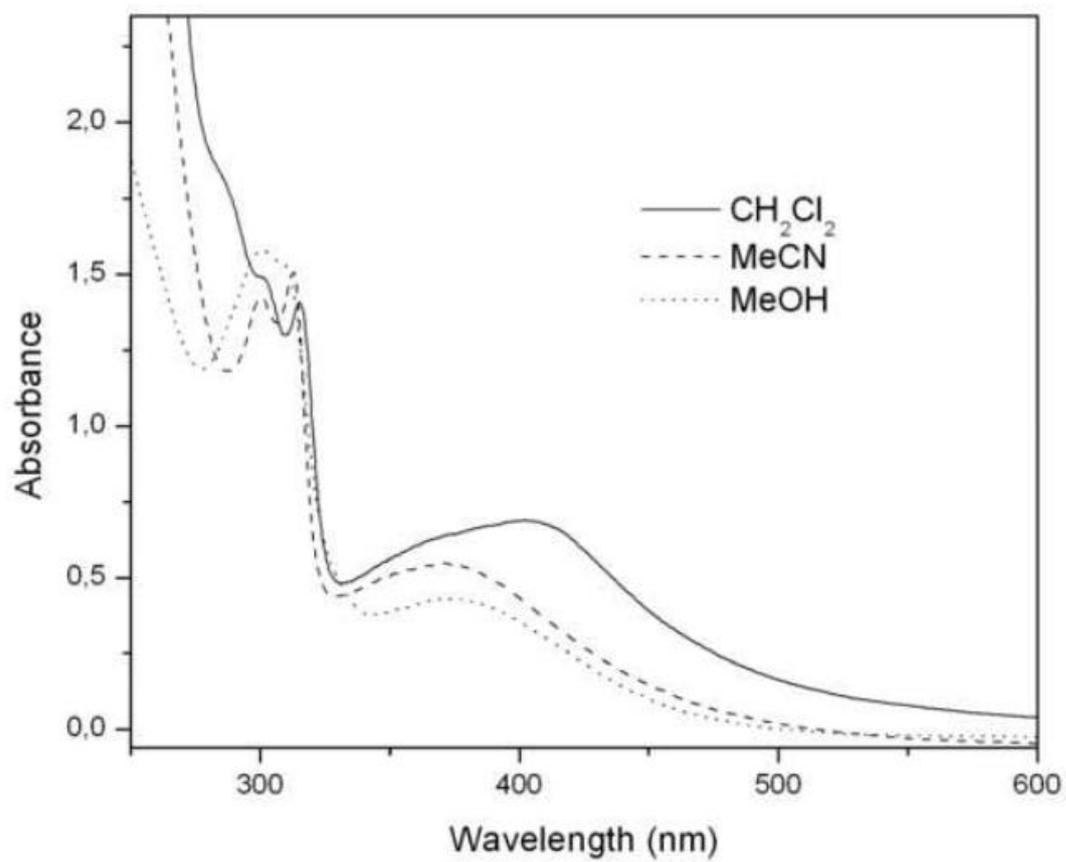
Fig. 2
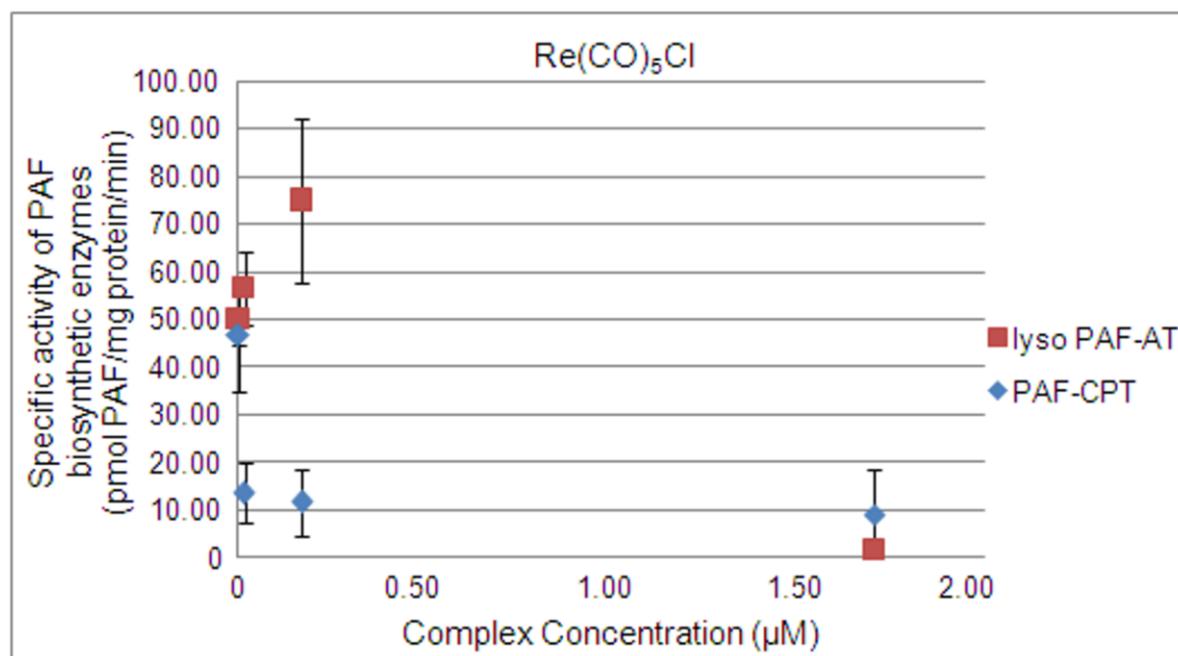
Fig. 3
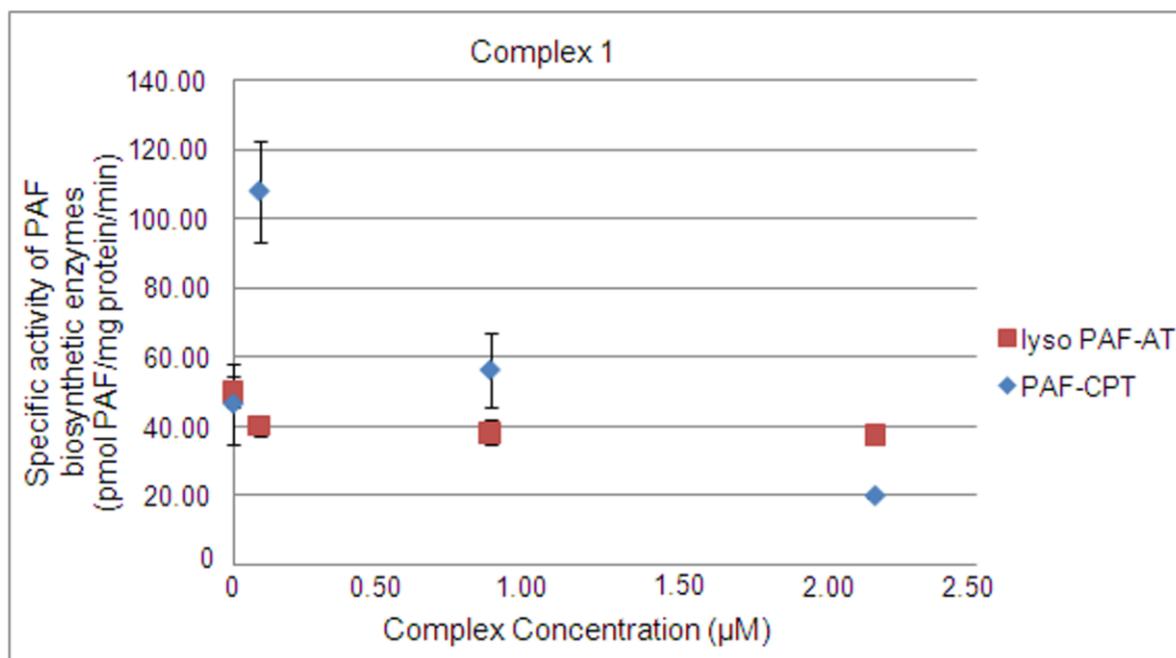
Fig. 4
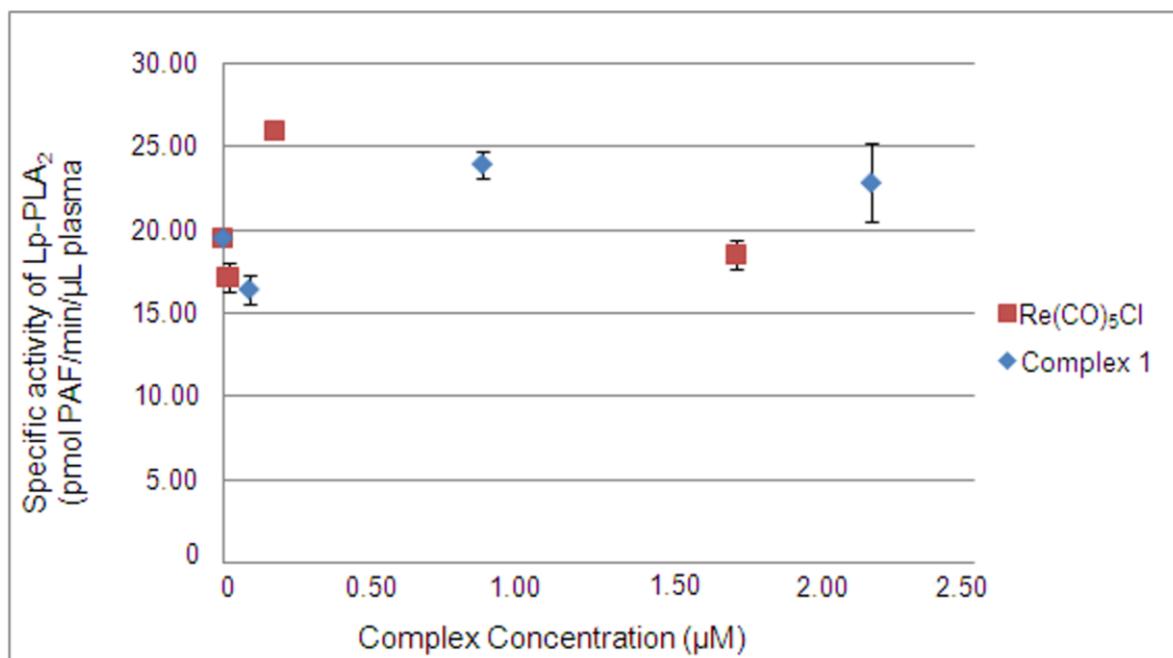
Fig. 5

33

Fig. 6

34

Fig. 7

Fig. 8

36
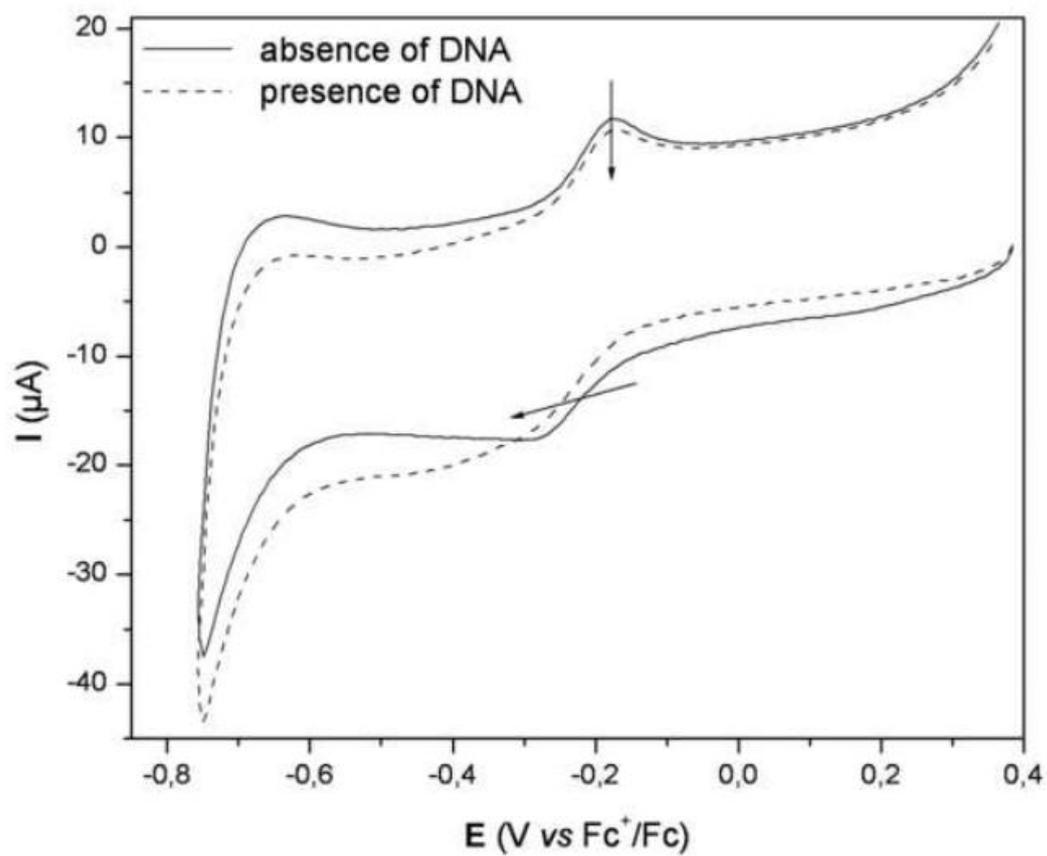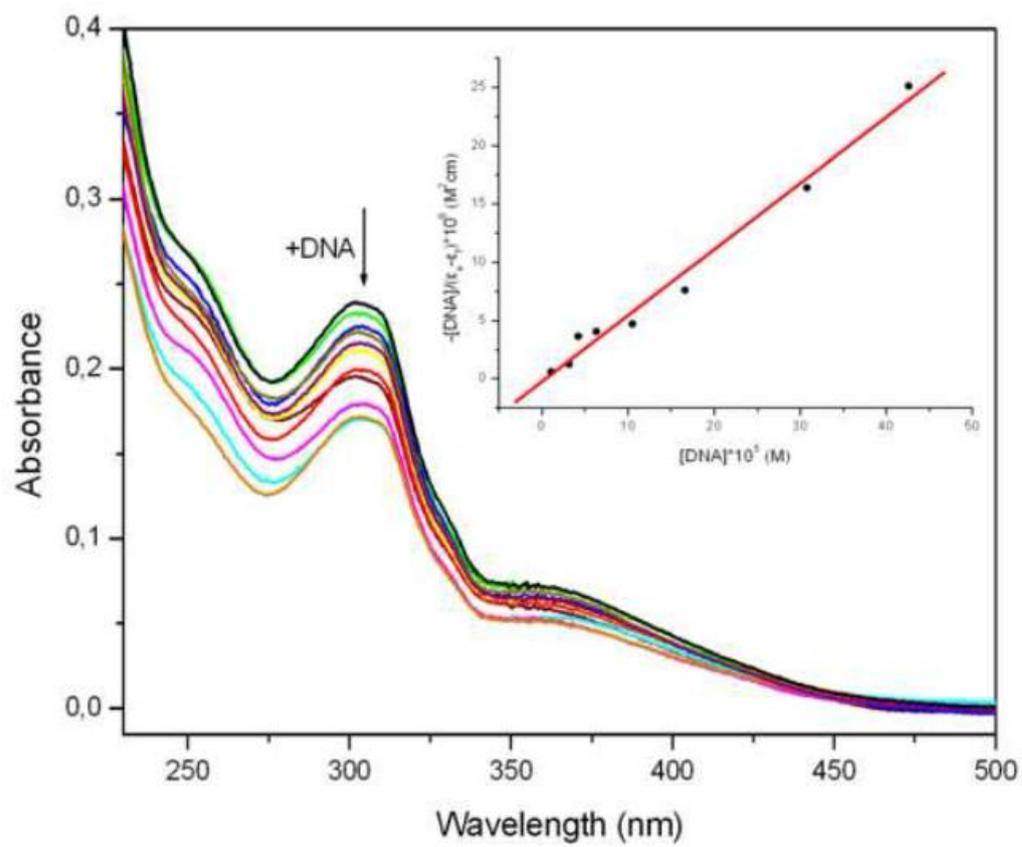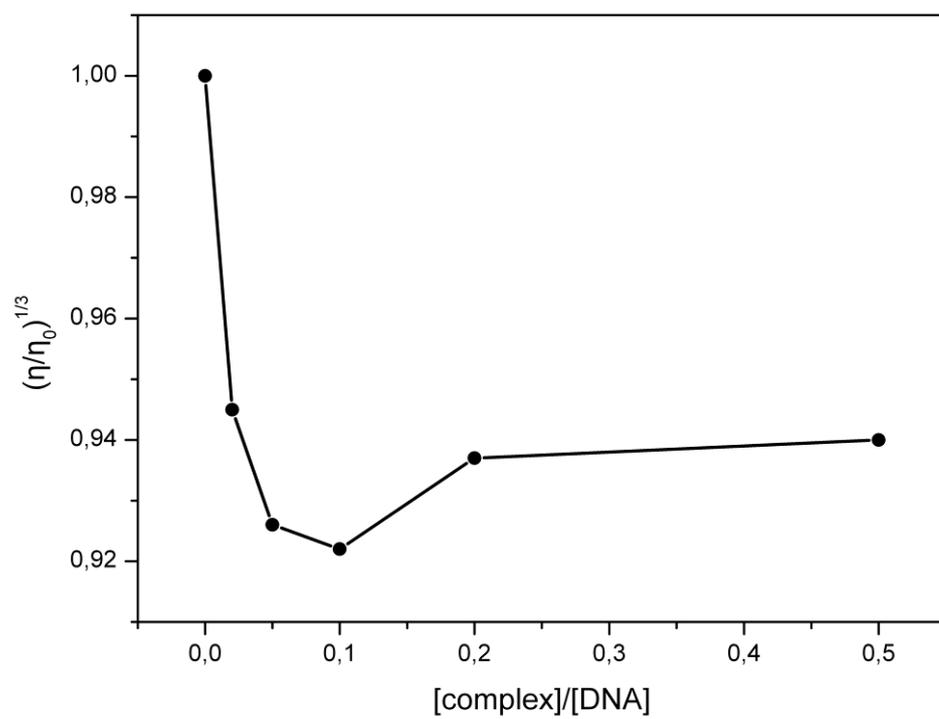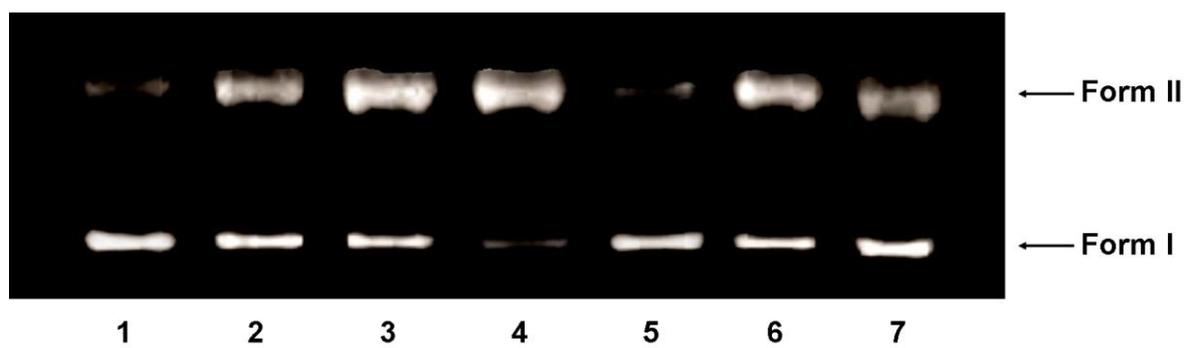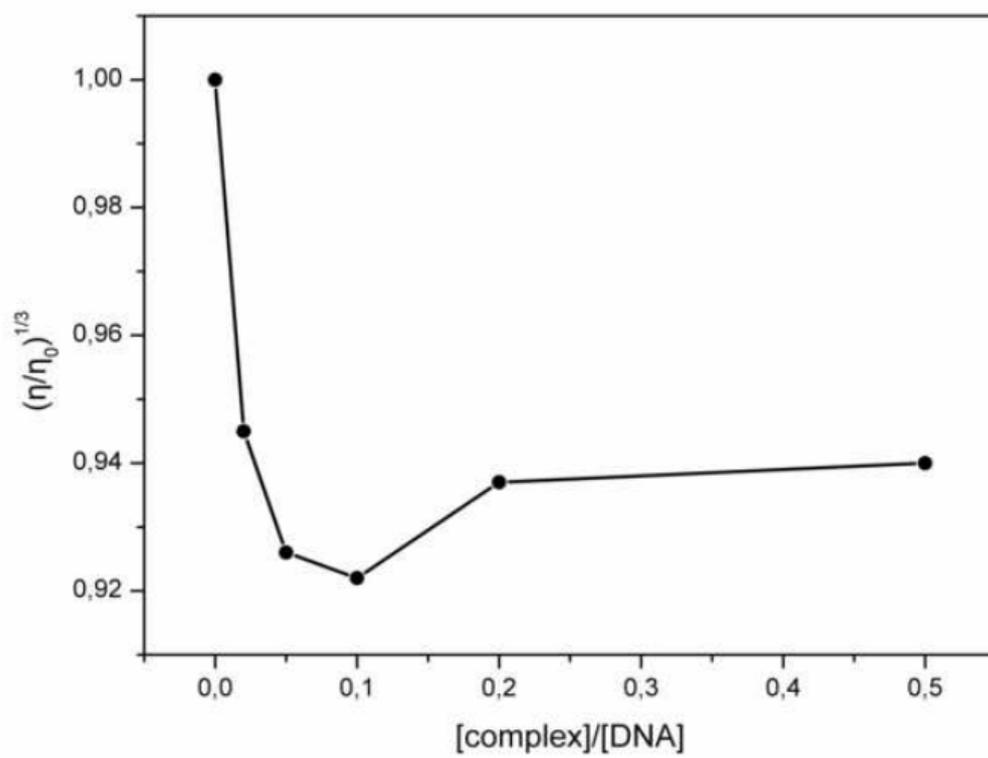
Fig. 9

Fig. 10

Highlights:

- A Re(I) complex of 1,10-phendione (**1**) was synthesized and fully characterized
- This complex binds to the major groove of DNA
- The [Re(CO)$_5$Cl**]** is potential inhibitor of PAF whereas **1** reduces PAF catabolism.
- The ground state of **1**exhibits medium anticancer activity
- Complex **1** photocleaves DNA via a proton coupled electron transfer mechanism